AD A058194

AFML-TR-77-29

LEVEL

IMPACT OF SOFT BODIES ON JET ENGINE FAN BLADES

UNIVERSITY OF DAYTON RESEARCH INSTITUTE
300 COLLEGE PARK
DAYTON, OHIO 45469

AD No. ____
DDC FILE COPY

APRIL 1977

DDC
RECEIVED
AUG 30 1978
A

TECHNICAL REPORT AFML-TR-77-29
Interim Report for the Period January 1976 – June 1976

Approved for public release; distribution unlimited.

AIR FORCE MATERIALS LABORATORY
AIR FORCE WRIGHT AERONAUTICAL LABORATORIES
AIR FORCE SYSTEMS COMMAND
WRIGHT-PATTERSON AIR FORCE BASE, OHIO 45433

8 08 21 061

NOTICE

When Government drawings, specifications, or other data are used for any purpose other than in connection with a definitely related Government procurement operation, the United States Government thereby incurs no responsibility nor any obligation whatsoever; and the fact that the government may have formulated, furnished, or in any way supplied the said drawings, specifications, or other data, is not to be regarded by implication or otherwise as in any manner licensing the holder or any other person or corporation, or conveying any rights or permission to manufacture, use, or sell any patented invention that may in any way be related thereto.

This report has been reviewed and cleared for open publication and/or public release by the appropriate Office of Information (OI) in accordance with AFR 190-170 and DODD 5230.9. There is no objection to unlimited distribution of this report to the public at large or by DDC to the National Technical Information Service (NTIS).

This technical report has been reviewed and is approved for publication.

James S Wilbeck

J. S. Wilbeck, Capt. USAF
Project Engineer

FOR THE COMMANDER

Lawrence N. Hjelm

LAWRENCE N. HJELM, Actg. Chief,
Metals Behavior Branch
Metals & Ceramics Division
Air Force Materials Laboratory

Copies of this report should not be returned unless return is required by security considerations, contractual obligations, or notice on a specific document.

AIR FORCE/56780/28 June 1978 — 300

UNCLASSIFIED

SECURITY CLASSIFICATION OF THIS PAGE *(When Data Entered)*

REPORT DOCUMENTATION PAGE

READ INSTRUCTIONS BEFORE COMPLETING FORM

1 REPORT NUMBER: AFML-TR-77-29	2 GOVT ACCESSION NO.
3 RECIPIENT'S CATALOG NUMBER	
4 TITLE (and Subtitle): IMPACT OF SOFT BODIES ON JET ENGINE FAN BLADES	5 TYPE OF REPORT & PERIOD COVERED: Interim Report 1 JAN [illegible] - 1 JUN [illegible]76
	6 PERFORMING ORG. REPORT NUMBER: UDRI-TR-76-33
7 AUTHOR(s): John P. Barber, John M. Klyce, Philip F. Fry, Henry R. Taylor	8 CONTRACT OR GRANT NUMBER(s): F33615-75-C-5152
9 PERFORMING ORGANIZATION NAME AND ADDRESS: University of Dayton Research Institute, 300 College Park, Dayton OH 45469	10 PROGRAM ELEMENT, PROJECT, TASK AREA & WORK UNIT NUMBERS: 62102F, 7351, 735106, 735106A1
11 CONTROLLING OFFICE NAME AND ADDRESS: Air Force Materials Laboratory (LLN), Wright-Patterson Air Force Base OH 45433	12 REPORT DATE: Apr[illegible]77
	13 NUMBER OF PAGES: 22
14 MONITORING AGENCY NAME & ADDRESS *(if different from Controlling Office)*	15 SECURITY CLASS *(of this report)*: UNCLASSIFIED
	15a DECLASSIFICATION/DOWNGRADING SCHEDULE

16 DISTRIBUTION STATEMENT *(of this Report)*

Approved for public release; distribution unlimited.

F33615-75-C-5052

17 DISTRIBUTION STATEMENT *(of the abstract entered in Block 20, if different from Report)*

18 SUPPLEMENTARY NOTES

19 KEY WORDS *(Continue on reverse side if necessary and identify by block number)*

Birds, Fan Blades, Jet Engines, Soft Body Impact, Impact (deg)

20 ABSTRACT *(Continue on reverse side if necessary and identify by block number)*

The momentum transferred to J-79 jet engine fan blades through impact with soft body projectiles was measured. Impacts onto stainless steel disks mounted normal to and 25° to trajectory were also investigated. Elementary analytical models of the momentum transfer were constructed for each of the three configurations.

DD FORM 1 JAN 73 1473 EDITION OF 1 NOV 65 IS OBSOLETE

UNCLASSIFIED

SECURITY CLASSIFICATION OF THIS PAGE *(When Data Entered)*

08 21 061

405 400

PREFACE

This report summarizes research conducted by the University of Dayton Research Institute at the Air Force Materials Laboratory, Wright-Patterson Air Force Base, Ohio under Phase II of Contract F33615-75-C-5052. This work was performed in conjunction with numerical studies conducted by California Research and Technology under subcontract to UDRI. The work by CRT was presented in AFML-TR-76-202.

The effort described was conducted in support of Project No. 7351 and Task No. 735106 for the Metals Behavior Branch, Metals and Ceramics Division, Air Force Materials Laboratory during the period January 1976 to June 1976. The contract monitor was Capt. James S. Wilbeck.

This report was submitted by the authors in January 1977 for publication as a Materials Laboratory Technical Report.

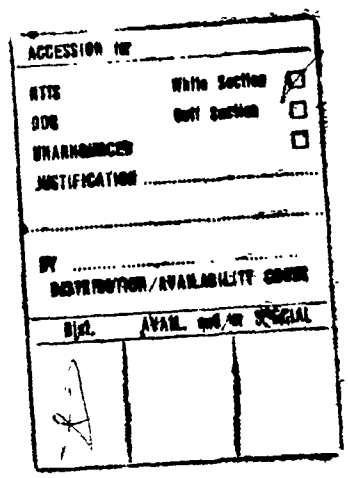

TABLE OF CONTENTS

LIST OF ILLUSTRATIONS

SECTION I
INTRODUCTION

The experiments conducted during this study were designed to measure the momentum transferred to pendulum mounted targets during impact with a soft body. Three target configurations were impacted: J-79 jet engine fan blades mounted 25° to trajectory and stainless steel disks mounted normal to and 25° to trajectory. The soft body projectiles were 4.4 cm diameter right circular gelatin cylinders 4.4 cm long.

The test conditions were chosen to coincide with the computer model being investigated by California Research and Technology (CRT). The major differences between the computer model and the experiment were the shape of and material used for the soft body projectile. The computer model of the projectile was a 5.46 cm diameter water sphere, whereas the projectile used for the experiments was a gelatin cylinder. No direct correlation between the computer model and experimental results was attempted in this report.

SECTION II
EXPERIMENTAL TECHNIQUE

2.1 MEASUREMENT OF MOMENTUM WITH A BALLISTIC PENDULUM

A ballistic pendulum as shown in Figure 1 can be used to accurately measure momentum transfer to a target. The projectile with momentum, mv, impacts a target mounted on the pendulum which is initially at rest. At impact, the projectile transfers momentum to the pendulum; $MV_o \sim m\Delta v$, where V_o is the initial velocity of the pendulum, M is the total mass of the pendulum, target and projectile if it is imbedded, and Δv is the change in projectile velocity. The energy of the target-pendulum is

$$MV^2/2 + Mgd = MV_o^2/2 \qquad (1)$$

where g is the acceleration of gravity, and d is the vertical displacement.

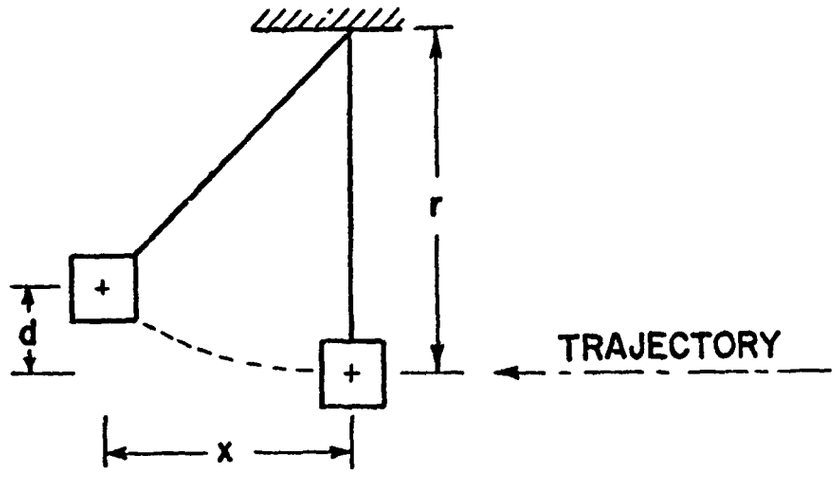

Figure 1. A schematic of a ballistic pendulum.

of the pendulum. Eq. (1) states that the total energy of the target-pendulum system (kinetic plus potential) is equal to the initial kinetic energy.

When the pendulum reaches the maximum vertical displacement, d_{max}, the velocity is momentarily zero and Eq. (1) leads to,

$$V_o = \sqrt{2gd_{max}} \ . \tag{2}$$

In practice, the horizontal displacement of the pendulum, x, is more easily and accurately measured than the vertical displacement, d. With reference to Figure 1, $r^2 = (r-d)^2 + x^2$, which can be rewritten as

$$d = \frac{x^2}{2r-d} \ , \tag{3}$$

and for d<<r:

$$d \approx x^2/2r. \tag{4}$$

Thus, the momentum transferred to the target-pendulum system can be calculated from MV_o (g/r). The momentum transfer is also related to the period of the pendulum, τ, which can be easily measured experimentally. For small angular displacements, $\tau = 2\pi\ (r/g)$. The momentum transferred to the target, P_t, may therefore, be determined from the period, mass, and horizontal displacement of the pendulum;

$$P_t = MV_o = 2\pi\ Mx/\tau. \tag{5}$$

2.2 DESIGN AND RELIABILITY OF PENDULUM

A five-wire ballistic pendulum was used to measure the momentum transferred to the target during impact. The pendulum is illustrated in Figure 2. The five-wire configuration eliminated all the rotational and all but two of the translational degrees of freedom of the pendulum. Motion was only permitted in the desired plane.

The mass of the pendulum was adjusted to maintain small angles of displacement (less than 5°) and thus preserve the small angle approximation

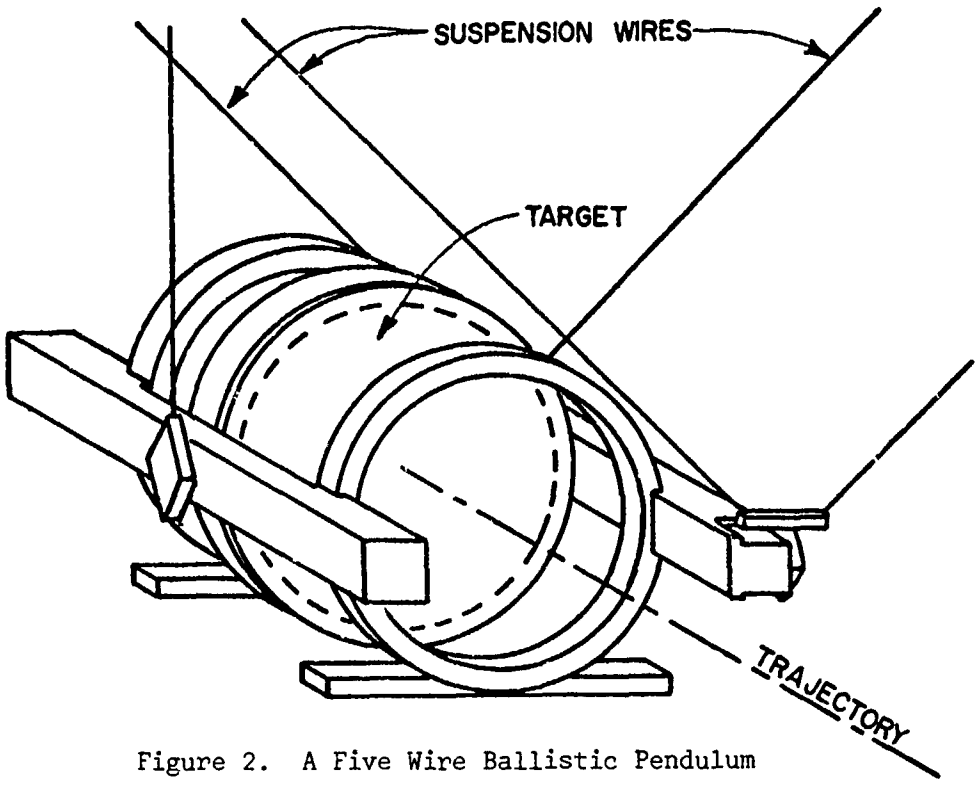

Figure 2. A Five Wire Ballistic Pendulum

necessary to facilitate data acquisition and reduction. The pendulum mass varied from 24.5 kg to 83.5 kg depending on the target configuration and angle of impact.

The pendulum period was measured with a spring trip wire actuated by the pendulum frame twice during each complete oscillation. The trip wire closed an electric circuit providing start/stop signals for an electronic counter. The period was determined to be 2.015.

A schematic of the pendulum displacement recording technique is shown in Figure 3. The displacement of the point light source attached to the pendulum was recorded with an open shutter Graflex camera. Figure 4 shows an example of a pendulum displacement record.

A reliability check of the ballistic pendulum was made by transferring a known momentum to the system and measuring the pendulum motion (shots 5566 and 5567). A projectile was launched into a tube mounted on the pendulum. As the projectile entered the tube, it struck and dislodged a doorstop, permitting the doors to close before the projectile could strike the closed tube end rebound to the entrance.

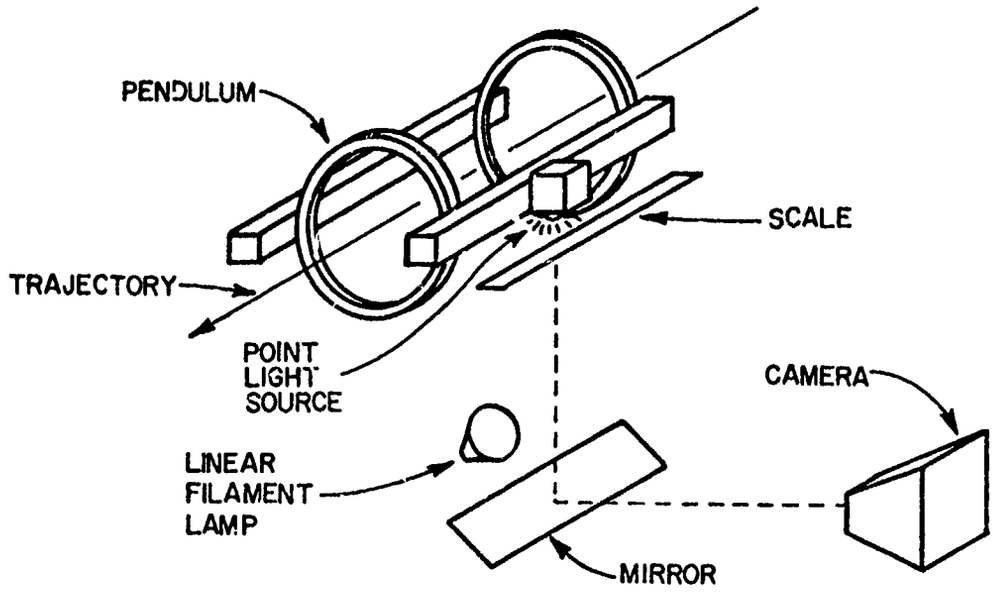

Figure 3. Illustration of pendulum movement recording technique.

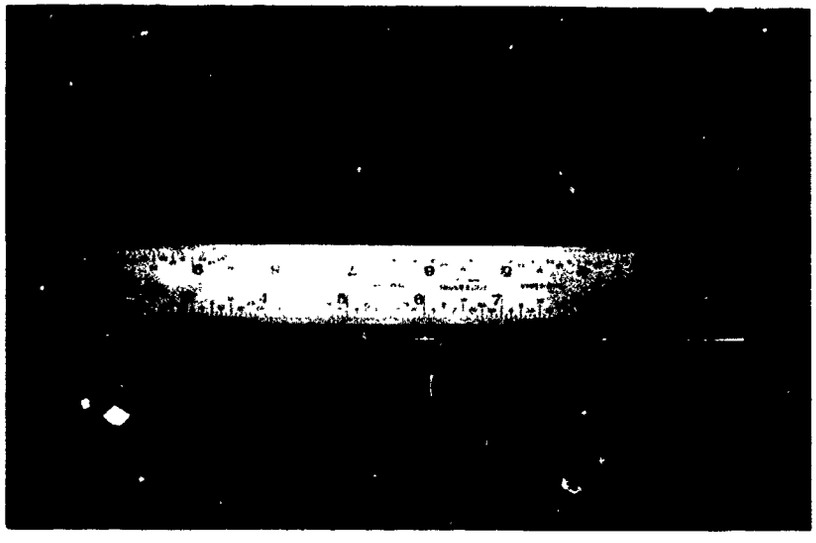

Figure 4. Typical pendulum movement record.

The results of this test, shown in Table 1 (at the end of Section III), indicate that the projectile momentum and the pendulum measured momentum agreed to within 2.0 percent. Therefore, the accuracy of the ballistic pendulum is considered to be within ±2.0 percent.

2.3 SOFT BODY LAUNCHER AND VELOCITY MEASUREMENT STATION

The soft body launcher had a 5.08 cm bore, 4.87 m long launch tube and was powered by compressed gas stored in a 0.32 m^3 steel tank. The tank was connected to the launch tube with a 10 cm diameter semiflexible hose and a quick disconnect coupling at the breech. The gun was fired by actuating a butterfly valve. A photograph of the breech end of the range and the compressed gas storage and delivery system is shown in Figure 5.

The sabot was a cylinder of balsa wood with a cavity to accept the projectile. A photograph of a cylindrical projectile mounted in a typical balsa wood sabot is shown in Figure 6. The sabot was stripped from the projectile by launching the sabot package into a 3 m long tapered tube which was slotted to permit escape of the driving gas. The sabot decelerated smoothly as it proceeded into the taper and was finally stopped.

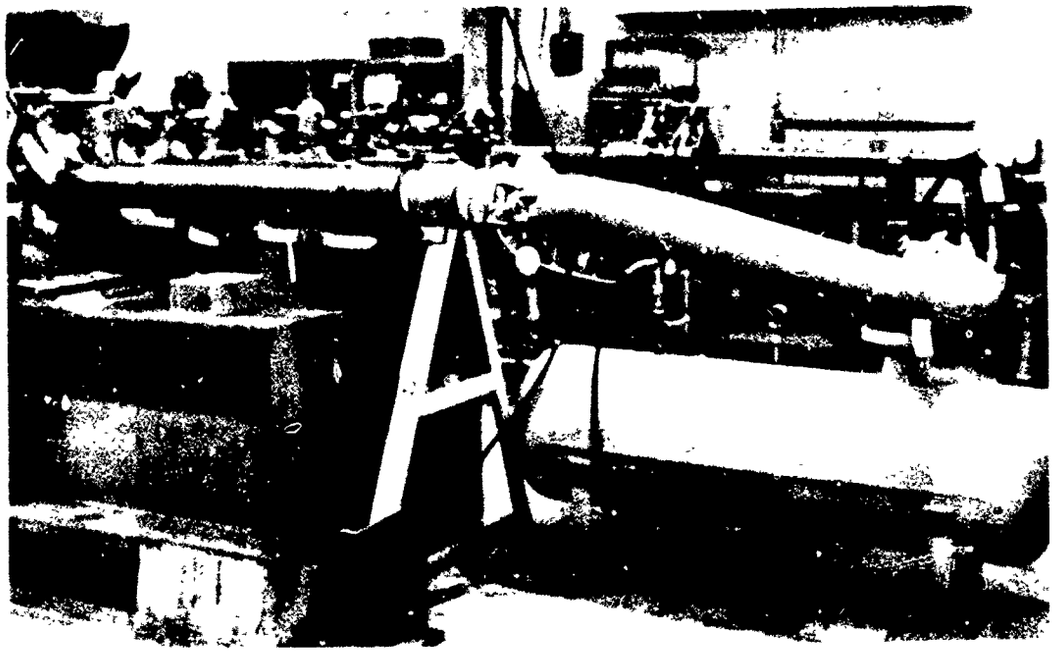

Figure 5. Breech end of range with compressed gas system.

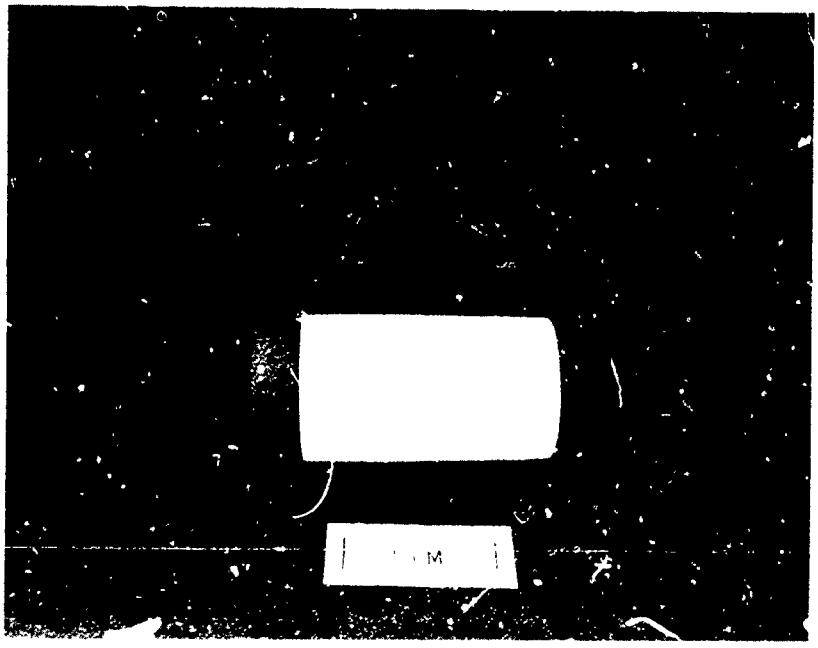

Figure 6. Cylindrical projectile with balsa wood sabot.

The projectile slipped from the sabot and continued on to the target. A photograph of the sabot stripper is shown in Figure 7.

The projectile velocity was determined by measuring the elapsed time between the interruption of the two HeNe laser beams. The laser beams were directed across the trajectory and onto the grids of photomultiplier tubes. The output of the photomultiplier tubes was monitored by an electronic time interval counter.

The projectile was photographed in free flight during each experiment to assess its integrity prior to impact. An example of a typical gelatin cylinder in free flight is shown in Figure 8.

2.4 PENDULUM MOUNTED TARGETS

The J-79 fan blades were cut to fit the target mount. Both ends of the blade section were rigidly mounted to the pendulum frame. The impact point was located in the center of the span and the chord of the blade was orientated at 25° to the projectile trajectory.

The 403 stainless steel disks (17.62 cm diameter x 3.55 cm thick) were simply-supported on a 15.2 cm ID tube which was fastened to the pendulum frame as shown in Figure 9.

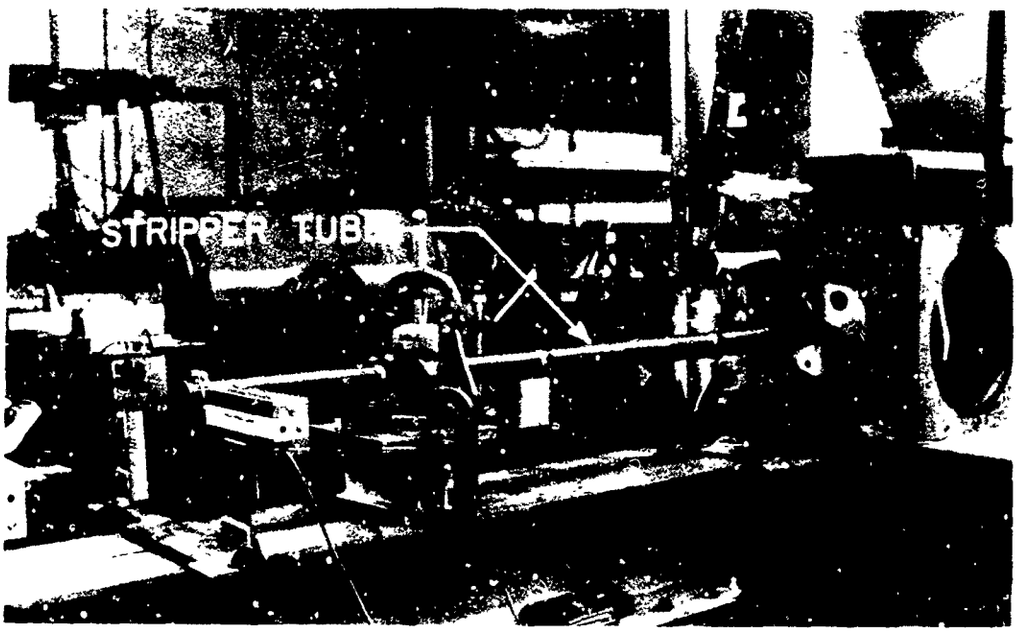

Figure 7. Sabot stripper.

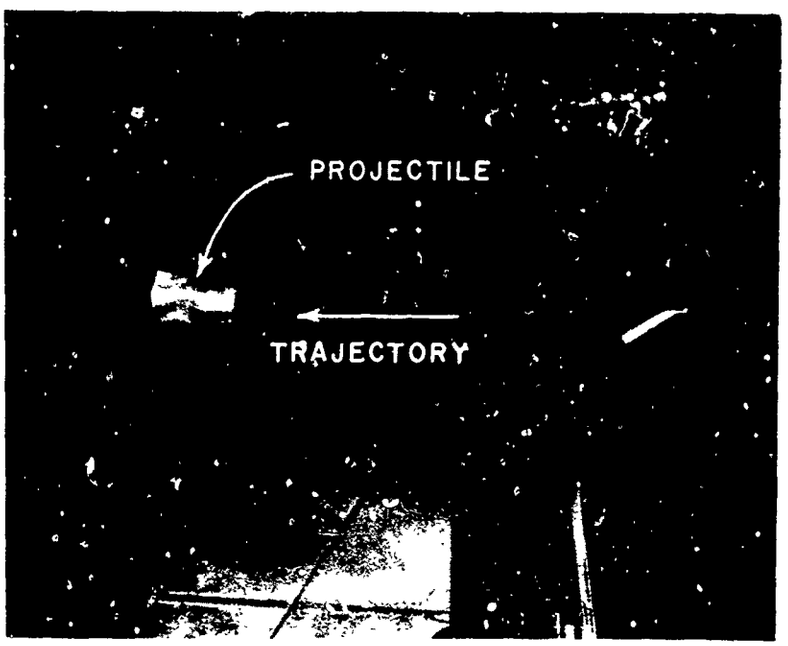

Figure 8. Gelatin cylinder in free flight.

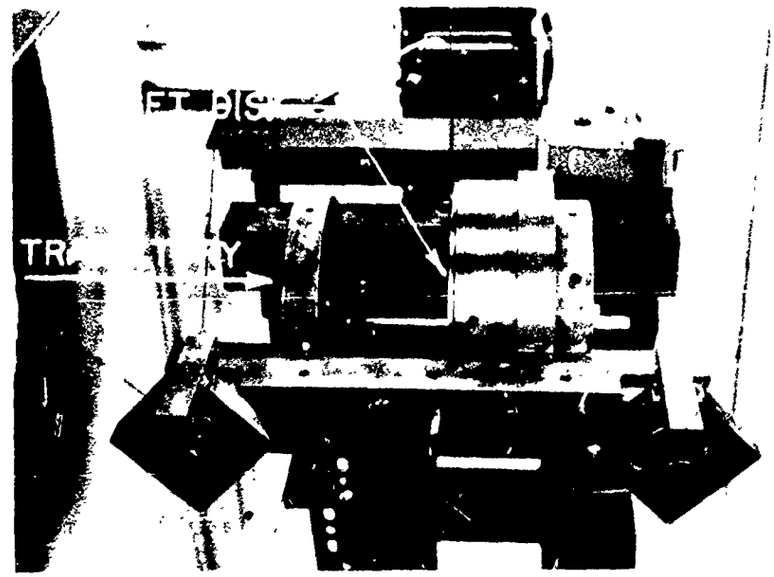

Figure 9. Disk target mounted normal to trajectory.

The disks were not clamped and the edges were free to rotate but not free to displace. Figure 10 shows an end-on view of the disk target mounted at 25° to trajectory. In all cases the target was bonded to the tube with double sided tape. Loosened screws were installed to restrain the target from flying off the pendulum after the impact.

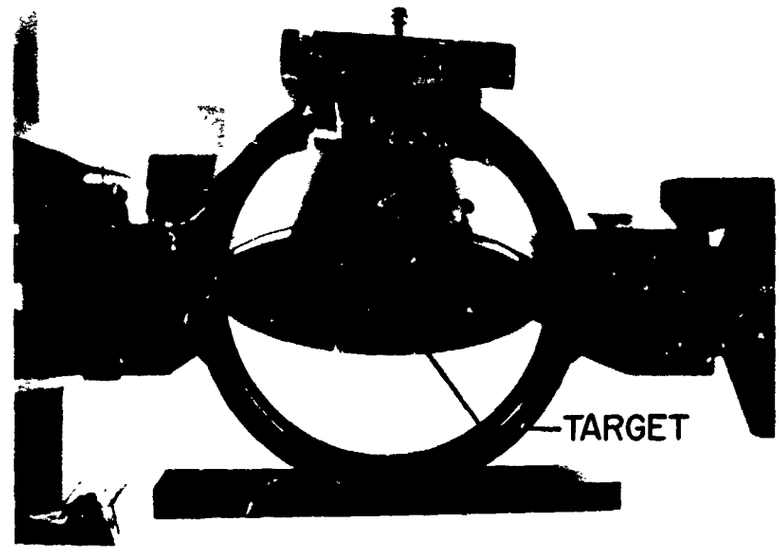

Figure 10. Disk target mounted 25° trajectory.

SECTION III
RESULTS

This section presents results of the test shots, elementary analytical models which describe these results and comparisons between the measured and calculated momentum transfers. Summaries of the raw and reduced data are contained in Tables 1 and 2 at the end of this section.

3.1 MOMENTUM TRANSFER MEASUREMENTS

The impacts investigated for this program simulated bird impacts onto jet engine fan blades. The objective was to measure the momentum transferred during impact with a soft body. All of the projectiles were gelatin cylinders. The gelatin projectiles were launched onto the blunt leading edge of J-79 fan blade sections and onto flat disks.

The target for shot 5568 was a boron-aluminum fan blade section. The impact forces broke the only available blade and due to the blade failure the recorded pendulum movement was not regarded as reliable. Reliable momentum transfer measurements were obtained for stainless steel blades which did not break. The target for shots 5573, 5575 and 5576 was a J-79 jet engine fan blade section fabricated from 403 stainless steel The target was mounted on the ballistic pendulum and impacted on the blunt leading edge with a gelatin cylinder as illustrated in Figure 11. The stainless steel fan blade was used repeatedly since it was only negligibly permanently deformed by each impact.

The gelatin cylinder was sliced during impact. The upper portion was recovered in one piece and the mass (m_α) was measured. The lower portion (with mass m_β) broke up and flowed along the bottom of the blade section. Since the upper portion of the projectile had very little interaction with the fan blade, all momentum transfer was attributed to the lower portion of the gelatin cylinder.

Flat disks were used as targets for shots 5593 through 5597. The 403 stainless steel disks were 0.36 cm thick and had 17.6 cm diameters. The disks were simply supported: the edges were free to rotate during impact but the

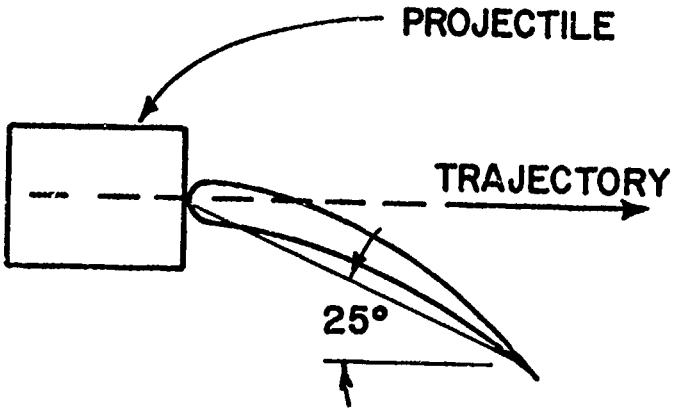

Figure 11. Impact onto blunt edge of fan blade.

disk was confined to the pendulum. Two test configurations were studied: the stainless steel disks were oriented at an angle of 90° to trajectory for three shots and at an angle of 25° to trajectory for two shots. The disks were impacted near the center. Profiles of the deformed disks were measured along the lines shown in Figure 12 and the angles of final deformation were measured from a plot of the disk profile as illustrated in Figure 13.

For shots 5593 through 5595, the stainless steel disks were mounted normal to trajectory as illustrated in Figure 14. During the impact process, the gelatin cylinder broke up and the target deformed plastically. The projectile flowed along the curved surface of the plate in a pattern that was symmetric about the trajectory. The total momentum transferred to the target was larger than the initial projectile momentum by 15 to 23 percent. Figure 15 is a photograph of a typical disk target that was impacted normal to trajectory.

For the last two shots, 5596 and 5597, the target was mounted at an angle of 25° to trajectory as illustrated in Figure 16. The projectile deformed and broke up during normal impact. The projectile was deflected downward and 24 to 26 percent of the projectile momentum was transferred to the target.

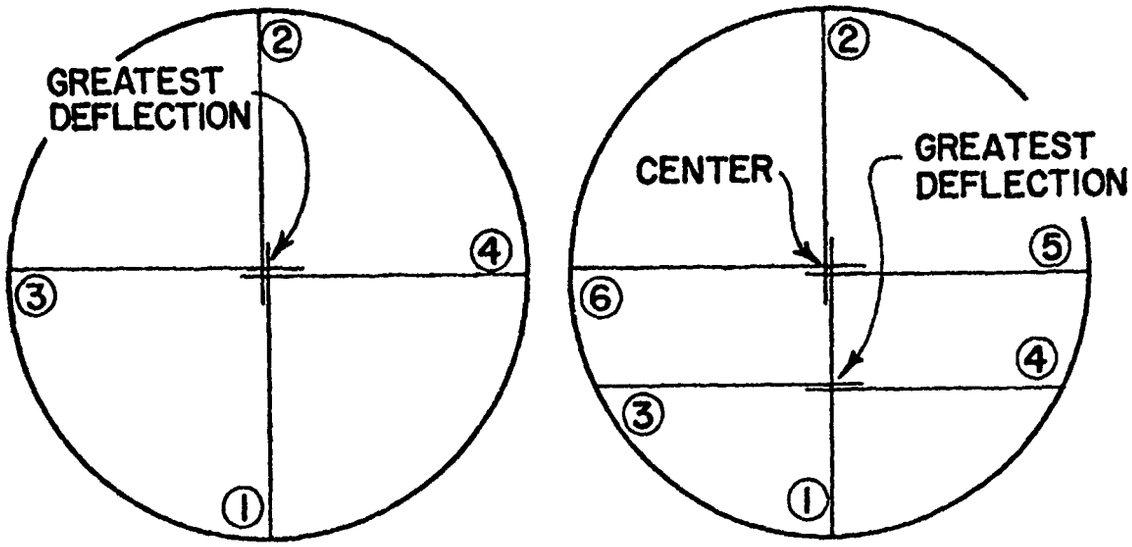

Figure 12. Schematic for lines used to map profiles of disks that deformed symmetrically and non-symmetrically.

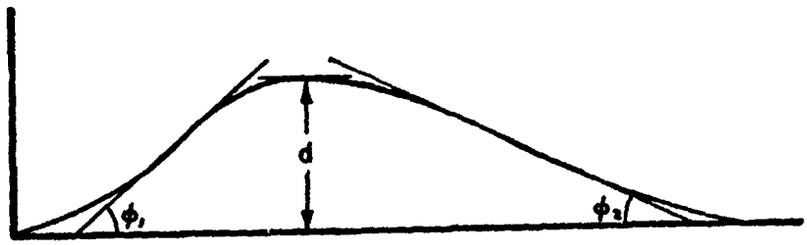

Figure 13. Schematic for measuring amount and angle of disk deformation for normal and oblique impacts.

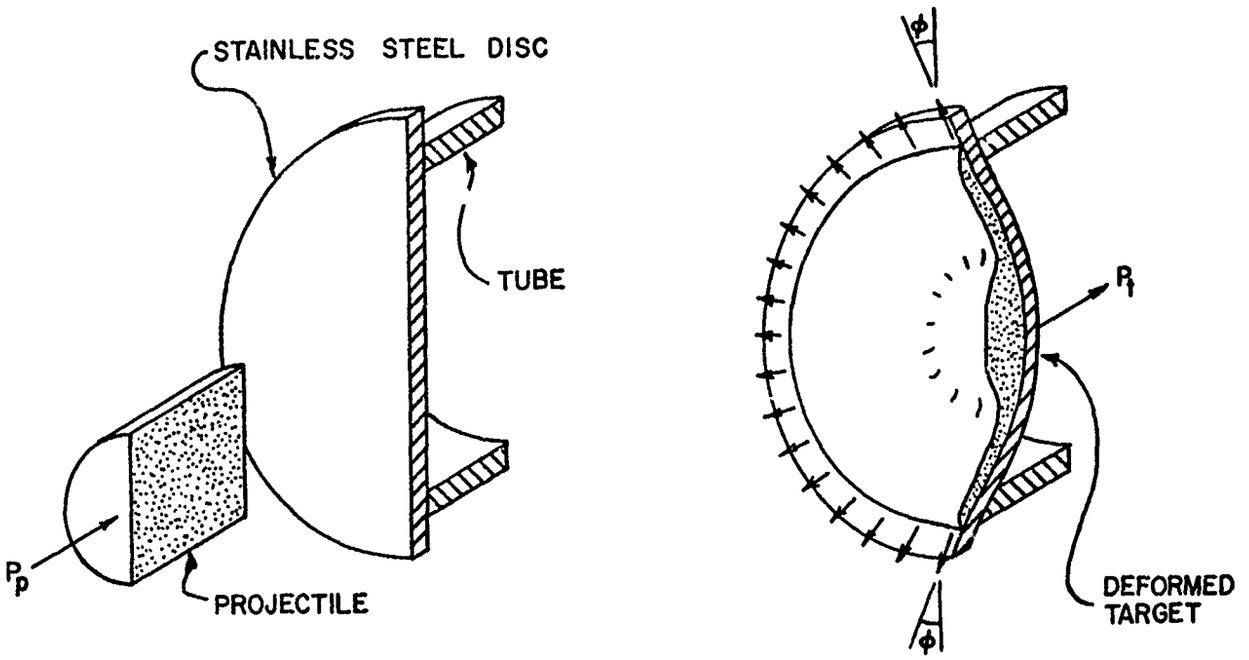

Figure 14. Impact onto disk mounted normal to trajectory.

Figure 15. A disk target impacted normal to trajectory.

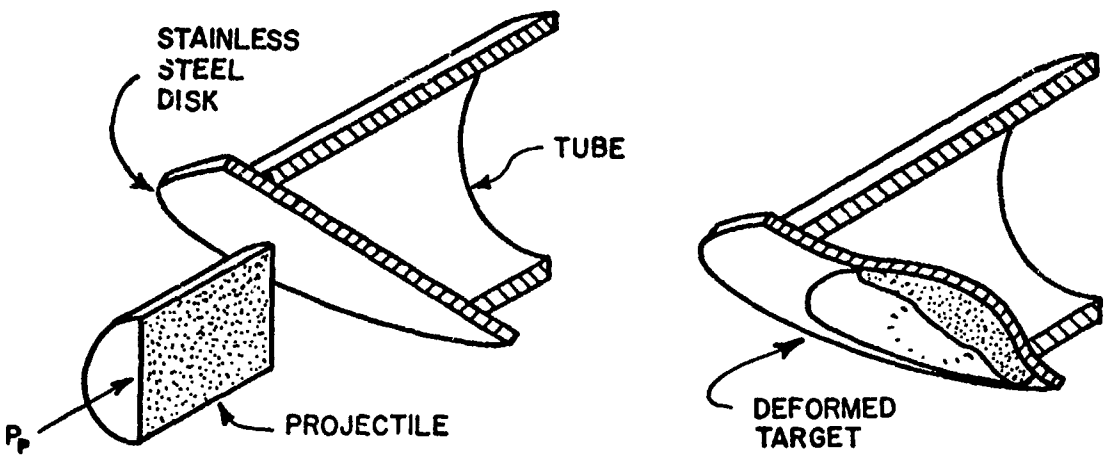

Figure 16. Impact onto disk mounted 25° to trajectory.

The disks did not deform symmetrically and the points of greatest deformation were below the initial impact point.

3.2 ANALYTICAL CALCULATIONS OF MOMENTUM TRANSFER

Models were developed for each impact condition; normal and oblique impacts onto the face of a deformable plate and impact onto a blunt, rigid plate edge. The most general case, impact onto a deformable target mounted at an angle to trajectory, degenerated to each of the other two models for the appropriate conditions. The models related the momentum transfer to the initial projectile momentum, the angle the plate surface originally made with the trajectory, θ, and the angle of final plate deflection, ϕ.

Two assumptions were required to develop the analytical model. The energy required to break up the projectile and the friction between the projectile and the target were neglected. Therefore, the first assumption was that the magnitude of the projectile velocity remained unchanged throughout the impact process. The diameter of the disk was large compared to both the diameter and length of the projectile, thus, the plate could reach

maximum deformation before the projectile flowed off the edge. Thus, the second assumption was that all of the projectile flowed off the edge. Thus, the second assumption was that all of the projectile flowed off of the deformed disk at the same angle. Further, the elastic deformation of the plate was considered to be small compared to the plastic deformation.

Consider the impact of a soft body onto a plate mounted perpendicular to the trajectory as depicted in Figure 14. The projectile impacts with momentum, mv, and all of this momentum is transferred to the target-pendulum system as shown in the momentum transfer diagram in Figure 17. The target deforms symmetrically to make an angle ϕ, with respect to the original plane of the plate. The projectile flows along the deforming surface, transferring additional momentum to the plate. Energy losses due to projectile break up and to friction with the plate are neglected. The projectile material is assumed to be ejected radially from the plate at angle ϕ, and speed v. Thus, the momentum, mv sin ϕ, is also transferred to the target. The total momentum transferred to the target is therefore,

$$P_t = mv\ (1 + \sin \phi). \tag{6}$$

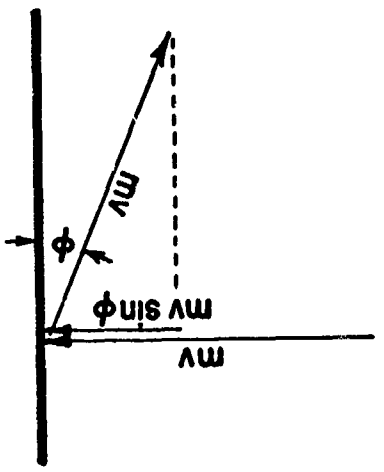

Figure 17. Momentum transfer diagram for soft body impact onto a deformable target mounted normal to trajectory.

In the second case, the target is initially mounted at angle θ to the trajectory as shown in Figure 16. The gelatin cylinder impacts and flows along the deforming target surface. The cylinder is then ejected along the target surface with no loss in velocity. The momentum transfer is illustrated in Figure 18. A portion of the projectile momentum is normal to the target, $mv \sin \theta$, and is transferred during impact. The pendulum reacts to only the horizontal component of the transferred momentum, $mv \sin^2 \theta$. The projectile flows along the deforming plate and is ejected downward at an angle of $(\theta + \phi)$ transferring additional momentum. The portion of this momentum sensed by the pendulum is the difference, $mv (\cos \theta - \cos (\theta + \phi))$. Thus, the momentum transferred by a soft projectile to a deformable target mounted oblique to trajectory and measurable by the pendulum is

$$P_t = mv [\sin^2\theta + \cos \theta - \cos (\theta + \phi)] \qquad (7)$$

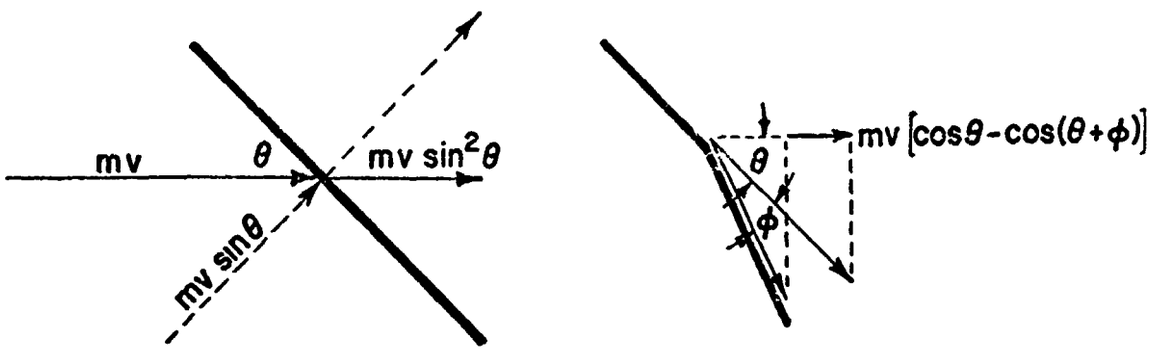

Figure 18. Momentum transfer diagram for soft body impact onto a deformable target mounted at angle to trajectory.

As θ approaches 90°, $\sin^2\theta$ approaches 1.0, cos θ approaches 0 and cos $(\theta + \phi)$ approaches -sin (ϕ). Thus Equation (7) reduces to Equation (6) for normal impact. If the target is rigid and does not deform, ϕ is zero and Equation (7) describes soft body impact onto a rigid plate.

The third case to consider is soft projectile impact onto the blunt edge of a rigid plate mounted at an angle to the trajectory as shown in Figure 19. This case simulates projectile impact onto the blunt leading edge of the J-79 fan blade illustrated in Figure 12. Part of the mass, m_β, is ejected downward along the surface of the plate and transfers a portion of its momentum to the plate. The remainder of the mass, m_α, sliced off at the leading edge, remains intact and continues over the disk without contributing significantly to the momentum transfer. Assuming the blade is a rigid body, ϕ is zero in Equation (7) and the momentum transfer, due only to the deflected portion of the projectile, is;

$$P_t = m \sin^2\theta. \tag{8}$$

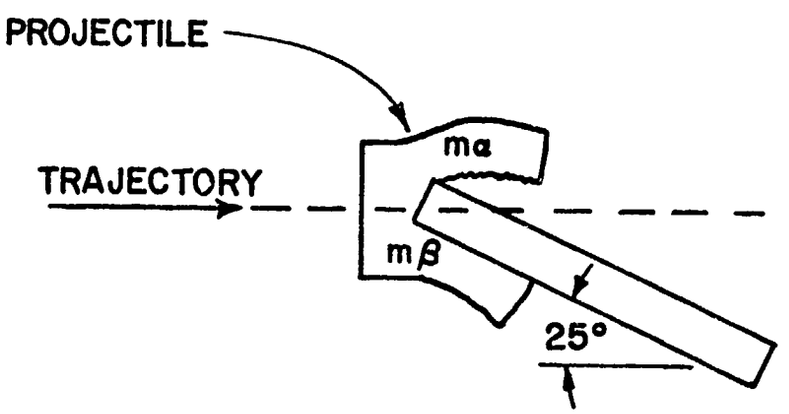

Figure 19. Schematic for soft body impact onto edge of a rigid plate (approximating blunt edge of fan blade).

In summary, the calculated ratios of transferred momentum to projectile momentum are given for three impact conditions:

center-of-plate

Normal: $$\frac{P_t}{P_p} = 1 + \sin \phi \tag{9}$$

center-of-plate

Oblique: $$\frac{P_t}{P_p} = \sin^2 \theta + \cos \theta - \cos (\theta + \phi) \tag{10}$$

blunt leading

edge: $$\frac{P_t}{P_p} = \frac{m_\beta}{m} \sin^2 \theta \tag{11}$$

3.3 COMPARISON BETWEEN MEASURED AND CALCULATED MOMENTUM TRANSFERS

The momentum transfer was measured with a ballistic pendulum to within 2.0 percent. The momentum transfer was also calculated from the elementary analytical models described in the previous section. The results are shown in Tables 1 and 2. The calculated values agreed well (within 4 percent) for the target mounted normal to trajectory. The analytical models did not provide good agreement for the targets mounted oblique to trajectory (differences of -16 and -21 percent). Agreement was onconsistent for the impact onto blunt leading edge of the J-79 fan blade (+13, -5, and -28 percent).

The magnitude and inconsistency of the discrepancies indicates that the elementary analytical models have limited use. The speeds at which the projectile slid off the disk were taken to be the magnitude of the impact velocities; and the masses that transferred momentum to the stainless steel J-79 fan blades were estimated to be those masses that could not be recovered. The errors in the calculated values of momentum transfer are directly proportional to errors in mass and velocity.

Calculations of momentum transfer are particularly sensitive to errors in θ and ϕ. For example, an error of 3° in θ leads to errors of 18° for oblique impacts of deformable targets and errors of 23° for impacts onto the blunt edge of rigid plates. Errors of 1° in knowledge of ϕ can lead to errors of nearly 4 percent in the calculated values of P_t.

TABLE 1. SUMMARY OF RAW DATA

Shot #	Target	Projectile Mass (g)	Velocity (m/s)	Projectile Momentum (kg·m/s)	Pendulum Mass (kg)	Pendulum Movement (cm)	m_α (g)	m_β (g)	ϕ (deg)	d (cm)
5566	Tube (trap)	84.5	208	17.6	77.20	7.30				
5567	Tube (trap)	80.2	214	17.2	77.20	7.02				
5568	B'11 J-79 blade (25°)	63.5	230	14.6	24.46	Blade Broke				
5573	SSJ-79 blade (25°)	71.5	202	14.4	24.46	2.42	36	35.5		
5575	SSJ-79 blade (25°)	71.1	212	15.1	24.46	2.54	23.5	47.6		
5576	SSJ-79 blade (25°)	73.0	198	14.5	24.46	2.00	26.2	46.8		
5593	SS Disk (90°)	68.2	218	14.9	83.54	6.68			9.4	1.45
5594	SS Disk (90°)	74.8	211	15.8	58.98	10.54			10.7	1.64
5595	SS Disk (90°)	75.0	200	15.0	18.53	6.81			10.3	1.49
5596	SS Disk (25°)	73.3	205	15.0	28.88	4.36			3.5	0.35
5597	SS Disk (25°)	72.6	201	14.6	28.88	3.93			3.1	0.30

ϕ = angle of deformation

for $\theta = 90°$, ϕ is an average of 4 readings.
for $\theta = 25°$, ϕ is measured along this line of projectile ejection.

d = maximum deformation of the target

m_α = undeflected portion of projectile mass

m_β = deflected portion of projectile mass

TABLE 2. SUMMARY OF REDUCED DATA

Shot #	Target	P_t (measured) (kg·m/s)	$\frac{P_t \text{ (measured)}}{P_p}$ (%)	P_t (calculated) (kg·m/s)	$\frac{P_t \text{ (calculated)}}{P_p}$ (%)	$\frac{P_t \text{ (calculated)}}{P_t \text{ (measured)}}$
5566	Tube (Trap)	17.6	100.0	17.6	NA	1.00
5567	Tube (Trap)	16.9	98.3	17.2	NA	1.02
5573	SSJ-79 blade (25°)	1.8	12.3	1.3	9.0	0.72
5575	SSJ-79 blade (25°)	1.9	12.6	1.8	11.9	0.95
5576	SSJ-79 blade (25°)	1.5	10.3	1.7	11.7	1.13
5593	SS Disk (90°)	17.9	120.	17.3	116.0	0.97
5594	SS Disk (90°)	19.4	123.	18.7	118.0	0.96
5595	SS Disk (25°)	17.3	115.	17.7	118.0	1.02
5596	SS Disk (25°)	3.93	26.2	3.10	20.7	0.79
5597	SS Disk (25°)	3.54	24.2	2.96	20.3	0.84

P_p = momentum of projectile

P_t = momentum transferred to target

SECTION IV
SUMMARY AND CONCLUSIONS

The momentum transferred to J-79 jet engine fan blades through impact with soft body projectiles was measured. Impacts onto stainless steel disks mounted normal to and 25° to trajectory were also investigated. Elementary analytical models of the momentum transfer were constructed for each of the three configurations. Calculated values of the momentum transfer were within 4 percent of the measured values for targets mounted normal to trajectory. Momentum transfer calculations for projectile impacts onto plates mounted at 25° to trajectory disagreed with the measured values by 16 and 21 percent. Calculations for momentum transfer for soft body impact onto the blunt edge of J-79 fan blades disagreed with the measured values by 5, 13, and 28 percent. These discrepancies are attributed principally to errors in the measurements of the plate deformation, ϕ.

REFERENCES

1. Rosenblatt, M., Eggum, G.E., DeAngelo, L.A., Kreyenhagen, K.N., Numerical Analyses of Soft Body Impacts on Rigid and Deformable Targets, AFML-TR-76-202, December 1976.

☆U.S.Government Printing Office: 1978 — 757-080/745